physica status solidi b
www.pss-b.com

basic solid state physics

Chiral and non-chiral p-wave superconducting states from correlated hopping interactions

J. S. Millán[1], L. A. Pérez[2], and C. Wang*[,3]

[1] Facultad de Ingeniería, Universidad Autónoma del Carmen, Cd. del Carmen, C.P. 24180, Campeche, Mexico
[2] Instituto de Física, Universidad Nacional Autónoma de México, A.P. 20-364, C.P. 01000, D.F., Mexico
[3] Instituto de Investigaciones en Materiales, Universidad Nacional Autónoma de México, A.P. 70-360, C.P. 04510, D.F., Mexico

Understanding anisotropic superconductivity has been one of the major theoretical challenges in the solid state physics. In this paper, we report a comparative study of chiral and non-chiral p-wave superconducting states by means of a generalized Hubbard Hamiltonian within the BCS formalism. The single-electron parameters were obtained by fitting *ab initio* band structure data supported by de Haas–van Alphen measurements in Sr_2RuO_4 and the electron correlation parameter was determined by the experimental critical temperature (T_c). This study was carried out by looking at T_c, superconducting gap, Helmholtz free energy, and electronic specific heat. The results show that both chiral and non-chiral p-wave superconducting states possess the same T_c but different superconducting energy gaps. Moreover, both states have almost the same Helmholtz free energy, which leads to their possible coexistence. Finally, the calculated electronic specific heats without adjustable parameters for both p-wave superconducting states are compared with the experimental data obtained from Sr_2RuO_4, observing a better agreement for the non-chiral case for temperatures much lower than T_c.

1 Introduction Five decades after the BCS theory, pairing mechanism in unconventional superconductors remains controversial. In these superconductors, the gap amplitude depends on the electron wave vector ($\boldsymbol{k}$) and its average over the Fermi surface is zero [1]. In particular, d-wave spin-singlet superconducting states were found in most high-T_c cuprate superconductors, whose pair wave function has lobes along $\pm x$ with opposite sign to lobes along $\pm y$ [2]. In particular, the presence of gap nodal lines gives rise to power-law behavior in low-temperature electronic specific heat, instead of the exponential one for the s-wave case. During the last years, the experimental evidence favors a spin-triplet superconducting state in Sr_2RuO_4, including phase sensitive measurements, which indicate an odd parity superconducting state, most likely of the p-wave type [3]. However, there is a controversy on the nature of this p-wave superconducting state in Sr_2RuO_4 [4], since spin-triplet states can be chiral or non-chiral, according to whether they break or not the time reversal symmetry [1].

On the other hand, Sr_2RuO_4 is structurally similar to $La_{2-x}Ba_xCuO_4$ and the electrons on RuO_2 planes are expected to play a dominant role in the superconducting transition [1]. The dynamics of these electrons can be described by a single-band square-lattice Hubbard model, which is often called γ band and the pairing on the other two bands, α and β, is induced passively through the inter-orbit couplings [5]. In concordance to the recent de Haas–van Alphen experiments, the band structure obtained from the density functional theory can be reasonably well described in the vicinity of the Fermi level by a single-band tight-binding model with first- and second-neighbor hopping $t = 0.4\,eV$ and $t' = 0.16\,eV$, respectively [6]. In general, the $k_x \pm k_y$ oriented p-wave superconducting states are doubly degenerated in a square lattice and a small distortion [7] in its right angles breaks this degeneracy, favoring one of the p-wave states in competition with s- and d-wave superconducting states [8]. We have found that the second-neighbor correlated-hopping interaction (Δt_3) is essential in p- and d-wave superconductivity, despite its relative small

magnitude of 0.1 eV for 3d electrons in transition metals in comparison with other interaction terms such as the on-site Coulomb interaction $U \sim 20\,\text{eV}$ in the same systems [9]. In this paper, we report a comparative study of the critical temperature (T_c), superconducting gap and electronic specific heat for chiral and non-chiral p-wave superconducting states by means of a single-band generalized Hubbard model containing nearest (t) and next-nearest neighbor (t') hoppings, correlated-hopping interactions between second neighbors (Δt_3), in addition to on-site (U) Coulomb interactions.

2 The model Let us start from the following generalized Hubbard Hamiltonian [8]

$$\hat{H} = t \sum_{<i,j>,\sigma} \hat{c}_{i\sigma}^+ \hat{c}_{j\sigma} + t' \sum_{\ll i,j \gg,\sigma} \hat{c}_{i\sigma}^+ \hat{c}_{j\sigma} + U \sum_{i,\sigma} \hat{n}_{i\sigma} \hat{n}_{i\bar{\sigma}}$$
$$+ \Delta t_3 \sum_{\substack{\ll i,j \gg,\sigma \\ <i,l>,<j,l>}} \hat{c}_{i\sigma}^+ \hat{c}_{j\sigma} \hat{n}_l, \tag{1}$$

where $\hat{n}_i = \hat{n}_{i\uparrow} + \hat{n}_{i\downarrow}$, $\hat{n}_{i\sigma} = \hat{c}_{i\sigma}^+ \hat{c}_{i\sigma}$, $\hat{c}_{i\sigma}^+$ ($\hat{c}_{i\sigma}$) is the creation (annihilation) operator with spin $\sigma = \downarrow$ or $\uparrow$ at site i, $\langle i,j \rangle$, and $\langle\langle i,j \rangle\rangle$, respectively, denote first and second neighbor sites in a square lattice with lattice parameter a. If we also consider a small distortion of the lattice right angles in order to include the possible existence of a bulk structural distortion in Sr_2RuO_4, the second-neighbor interactions, such as t' and Δt_3 respectively change to $t'_\pm = t' \pm \delta$ and $\Delta t_3^\pm = \Delta t_3 \pm \delta_3$, where $\pm$ refers to the $x \pm y$ direction.

In order to keep the minimal number of parameters, we choose $\Delta t_3 = \delta = 0$ since Δt_3 and δ do not generate p-wave superconductivity [10]. They only have an indirect effect through the mean-field dispersion relation by changing the effective second-neighbor hopping strength. However, such change does not affect the conclusions of this study. In this case, Hamiltonian (1) can be written in the momentum space as [8]

$$\hat{H} = \sum_{k,\sigma} \varepsilon_0(\boldsymbol{k}) \hat{c}_{k,\sigma}^+ \hat{c}_{k,\sigma} + \frac{1}{N_s} \sum_{k,k'} V_{k,k'} \hat{c}_{k+q,\uparrow}^+ \hat{c}_{-k'+q,\downarrow}^+ \hat{c}_{-k'+q,\downarrow} \hat{c}_{k+q,\uparrow}$$
$$+ \frac{1}{N_s} \sum_{k,k',\sigma} W_{k,k',q} \hat{c}_{k+q,\sigma}^+ \hat{c}_{-k'+q,\sigma}^+ \hat{c}_{-k'+q,\sigma} \hat{c}_{k+q,\sigma}, \tag{2}$$

where N_s is the total number of sites,

$$\varepsilon_0(\boldsymbol{k}) = 2t \big[\cos(k_x a) + \cos(k_y a)\big] + 4t' \cos(k_x a) \cos(k_y a), \tag{3}$$

$$V_{k,k',q} = U + \delta_3[\gamma(\boldsymbol{k}+\boldsymbol{q},\boldsymbol{k}'+\boldsymbol{q}) + \gamma(-\boldsymbol{k}+\boldsymbol{q}, -\boldsymbol{k}'+\boldsymbol{q})]$$
$$- \delta_3[\zeta(\boldsymbol{k}+\boldsymbol{q},\boldsymbol{k}'+\boldsymbol{q}) + \zeta(-\boldsymbol{k}+\boldsymbol{q},-\boldsymbol{k}'+\boldsymbol{q})], \tag{4}$$

and

$$W_{k,k',q} = \delta_3 \gamma(\boldsymbol{k}+\boldsymbol{q},\boldsymbol{k}'+\boldsymbol{q}) - \delta_3 \zeta(\boldsymbol{k}+\boldsymbol{q},\boldsymbol{k}'+\boldsymbol{q}), \tag{5}$$

being

$$\gamma(\boldsymbol{k},\boldsymbol{k}') = 2\cos(k_x a + k'_y a) + 2\cos(k'_x a + k_y a), \tag{6}$$

$$\zeta(\boldsymbol{k},\boldsymbol{k}') = 2\cos(k_x a - k'_y a) + 2\cos(k'_x a - k_y a), \tag{7}$$

and $2\boldsymbol{q}$ is the wave vector of the pair center of mass. After a standard Hartree–Fock decoupling [11] of the interaction terms in Eq. (2), the reduced Hamiltonian is obtained [8] by taking $\boldsymbol{q} = 0$ in Eq. (2) and replacing the dispersion relation $\varepsilon_0(\boldsymbol{k})$ of Eq. (3) by the mean-field one given by

$$\varepsilon(\boldsymbol{k}) = U\frac{n}{2} + 2t\big[\cos(k_x a) + \cos(k_y a)\big]$$
$$+ 2(t' + 2n\delta_3)\cos(k_x a + k_y a)$$
$$+ 2(t' - 2n\delta_3)\cos(k_x a - k_y a), \tag{8}$$

where the single electron dispersion relation $\varepsilon(\boldsymbol{k})$ is now modified by adding terms $Un/2$ and $\pm 2n\delta_3$ to the self-energy and the second-neighbor hopping integral t', respectively.

Applying the BCS formalism to Eq. (2), we obtain the following two coupled integral equations [12],

$$\begin{cases} \Delta_\alpha(\boldsymbol{k}) = -\dfrac{1}{N_s} \sum_{k'} \dfrac{Z_{k,k'} \Delta_\alpha(\boldsymbol{k}')}{2E_\alpha(\boldsymbol{k}')} \tanh\left(\dfrac{E_\alpha(\boldsymbol{k}')}{2k_B T}\right) \\[3mm] n - 1 = -\dfrac{1}{N_s} \sum_{k} \dfrac{\varepsilon(\boldsymbol{k}) - \mu_\alpha}{E_\alpha(\boldsymbol{k})} \tanh\left(\dfrac{E_\alpha(\boldsymbol{k})}{2k_B T}\right) \end{cases}, \tag{9}$$

where

$$Z_{k,k'} = \begin{cases} V_{k,k',0}, & \text{for pairs with } \dfrac{1}{\sqrt{2}}(|\uparrow\downarrow\rangle + |\downarrow\uparrow\rangle), \\[3mm] W_{k,k',0}, & \text{for pairs with } |\uparrow\uparrow\rangle \text{ or } |\downarrow\downarrow\rangle \end{cases}, \tag{10}$$

and the single excitation energy is given by

$$E_\alpha(\boldsymbol{k}) = \sqrt{[\varepsilon(\boldsymbol{k}) - \mu_\alpha]^2 + |\Delta_\alpha(\boldsymbol{k})|^2}, \tag{11}$$

being $\alpha = \text{c}$ for the chiral superconducting states with

$$\Delta_c(\boldsymbol{k}) = \Delta_c[\sin(k_x a) \pm i \sin(k_y a)] \tag{12}$$

or $\alpha = \text{nc}$ for the non-chiral case with

$$\Delta_{nc}(\boldsymbol{k}) = \Delta_{nc}[\sin(k_x a) \pm \sin(k_y a)]. \tag{13}$$

Equation (9) can be used to determine, for example, (a) the chemical potential (μ) and the superconducting gap $[\Delta(\boldsymbol{k})]$ for each given temperature (T) and electron concentration (n), or (b) μ and T_c for each n when the superconducting gap vanishes.

It is worth mentioning that the gap equation in (9) is the same for triplets with the three spin projections [8, 13, 14],

as well as for both chiral and non-chiral cases when the gap is zero. The latter can be proved by substituting Eqs. (12) and (13) into (9), leading to the same equation

$$1 = \pm \frac{2\delta_3}{N_s} \sum_{\boldsymbol{k'}} \frac{[\sin(k'_x a) \pm \sin(k'_y a)]^2}{E_\alpha(\boldsymbol{k'})} \tanh\left(\frac{E_\alpha(\boldsymbol{k'})}{2k_B T}\right),$$

(14)

which differs for chiral and non-chiral cases because

$$|\Delta_c(\boldsymbol{k})|^2 = (\Delta_c)^2[\sin^2(k_x a) + \sin^2(k_y a)]$$

(15)

and

$$|\Delta_{nc}(\boldsymbol{k})|^2 = (\Delta_{nc})^2[\sin(k_x a) \pm \sin(k_y a)]^2,$$

(16)

except for calculating T_c since $\Delta_\alpha = 0$.

On the other hand, the three site term in Eq. (1) is crucial for anisotropic superconductivity, since it promotes a change of sign of the pair wavefunction (φ) between second neighbor sites when it is written in the relative spatial coordinate ($\mathbf{r}$) representation [15]. In particular, second-neighbor interactions with a finite δ_3 produce p-symmetry pair wavefunctions [16] with $\varphi(\mathbf{r}) = -\varphi(-\mathbf{r})$ and a node at $\mathbf{r} = 0$, which make them insensitive to the onsite interaction (U). When a Fourier transform of $\varphi(\mathbf{r})$ is performed, we get a p-wave function in the momentum space with $\varphi(\boldsymbol{k}) = -\varphi(-\boldsymbol{k})$. Moreover, in the dilute limit we have $\varphi(\boldsymbol{k}) \sim \Delta(\boldsymbol{k})/E(\boldsymbol{k})$ [17] and then a p-wave superconducting gap.

3 Superconducting properties The single-particle Hamiltonian parameters $t = -0.4$ eV and $t' = -0.16$ eV are taken from Ref. [6]. The onsite Coulomb interaction parameter (U) has no effect on the p-wave superconducting states, within the BCS formalism [10]. In consequence, T_c is a function of n and δ_3. By requiring $T_c(n) = 1.5$ K as a maximum, we obtain $n = 0.9$ and $\delta_3 = 0.064$ eV. The numerical calculations were performed by using a multi-region integration method [18], i.e., by dividing the first Brillouin zone in several regions, which are separately integrated as shown in Fig. 1. This method allows an efficient calculation of the integrals of Eq. (9) since the integrand functions are extremely sharp around the Fermi surface, especially for small pairing interactions or low temperatures.

In Fig. 2a, the chiral and non-chiral superconducting gaps (Δ_α) and in Fig. 2b the critical temperature (T_c) are shown as functions of electronic density (n). Observe that both chiral and non-chiral symmetries have the same T_c but the chiral superconducting gap is larger than the non-chiral one.

There are analytical solutions for Eqs. (9) at $T = 0$ in the limit of low electronic density ($n \to 0$) and strong coupling [$\varepsilon(\boldsymbol{k}) \to 0$], as those obtained for non-chiral p-wave superconducting states [8]. In this limit, $\mu_\alpha < 0$
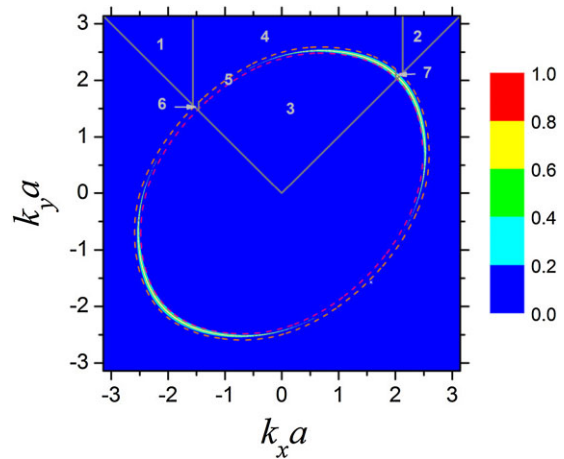

Figure 1 The integrand function of Eq. (14) with $T = T_c$ in color scale over the 1BZ for the non-chiral p-wave case. Pink and orange dashed lines indicate two contour lines obtained with $\varepsilon(\boldsymbol{k}) = 1.2\mu_{nc}$ and $\varepsilon(\boldsymbol{k}) = 0.85\mu_{nc}$ around the Fermi surface $\varepsilon(\boldsymbol{k}) = \mu_{nc}$, respectively. Seven integration regions in a fourth part of the 1BZ are illustrated.
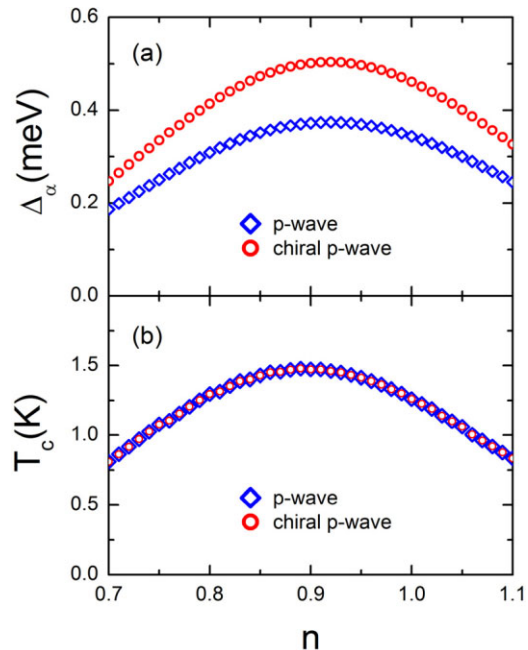

Figure 2 (a) Chiral (red open circles) and non-chiral (blue open rhombuses) superconducting gaps (Δ_α) at zero temperature and (b) critical temperatures (T_c) as functions of electronic density (n), for systems with $t = -0.4$ eV, $t' = -0.16$ eV, and $\delta = 0.064$ eV.

and

$$\frac{1}{E_\alpha(\boldsymbol{k})} \approx -\frac{1}{\mu_\alpha}\left[1 - \frac{|\Delta_\alpha(\boldsymbol{k})|^2}{2\mu_\alpha^2}\right],$$

(17)

as in Ref. [19]. Hence, the second equation of (9) gives $\Delta_\alpha = |\mu_\alpha|\sqrt{2n}$ and substituting it in Eq. (14) we obtain $\Delta_\alpha = 2\delta_3\sqrt{2n}(1 - \gamma_\alpha n)$, with $\gamma_c = 7/4$ and $\gamma_{nc} = 9/4$. Notice that the chiral superconducting gap (Δ_c) is larger than the non-chiral one (Δ_{nc}), in agreement with the numerical results.

Figure 3 shows the chiral and non-chiral superconducting gaps as a function of the temperature for systems with $t = -0.4\,\text{eV}$, $t' = -0.16\,\text{eV}$, $\delta_3 = 0.064\,\text{eV}$, and $n = 0.9$.

From these data, the electronic specific heat (C_α) can be calculated by using [20]

$$C_\alpha = \frac{2k_B\beta^2 a^2}{4\pi^2} \int\limits_{-\pi/a}^{\pi/a} \int\limits_{-\pi/a}^{\pi/a} f[E_\alpha(\boldsymbol{k})]\{1 - f[E_\alpha(\boldsymbol{k})]\}$$

$$\times \left[E_\alpha^2(\boldsymbol{k}) + \beta E_\alpha(\boldsymbol{k})\frac{dE_\alpha(\boldsymbol{k})}{d\beta}\right]dk_x dk_y \,.$$

$$(18)$$

where $\beta = 1/(k_B T)$ and $f(E)$ is the Fermi–Dirac distribution. The specific heat of the normal state can be obtained by taking $\Delta(\boldsymbol{k})$ equal to zero in Eqs. (11) and (18). Figure 4 shows the normalized electronic specific heat for both chiral and non-chiral superconducting gaps as functions of the temperature, in comparison with the experimental data of Sr_2RuO_4 from Ref. [21]. Observe that the non-chiral p-wave specific heat has a better agreement with the experimental results than the chiral one.

Moreover, Fig. 4 reveals that at very low temperatures the chiral p-wave electronic specific heat has an exponential behavior whereas the non-chiral one follows a power law. This is due to fact that the former has no nodes and the latter has a nodal line, as illustrated in Fig. 5 by means of the single-particle excitation energy gap $\left[\Delta_\alpha^{min}(\theta)\right]$ defined as the minimum value of $E(\boldsymbol{k})$ along the polar angle $\theta = \tan^{-1}(k_y/k_x)$.

In Fig. 5, notice also that $\Delta_{nc}^{min}(\pi/4) > \Delta_c^{min}(\pi/4)$, in spite of having $\Delta_c > \Delta_{nc}$ as shown in Fig. 3. This fact can be
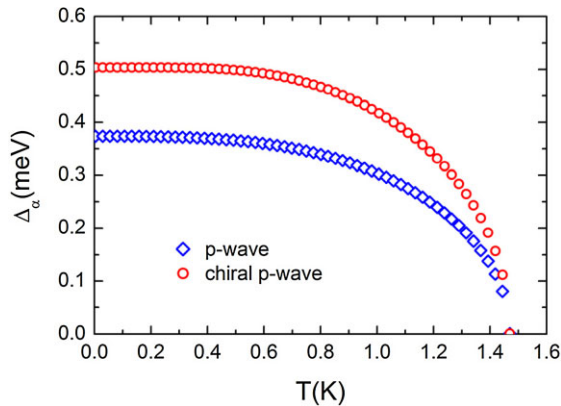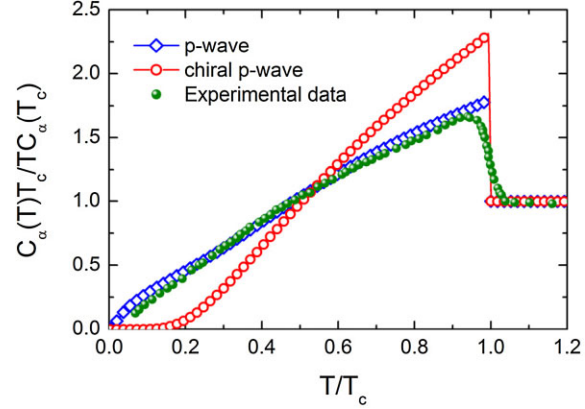

Figure 4 Normalized electronic specific heats (C_α) as functions of temperature (T) for chiral (open red circles) and non-chiral (open blue rhombuses) p-wave superconductors with the same parameters as in Fig. 3, in comparison with Sr_2RuO_4 experimental data (solid circles)
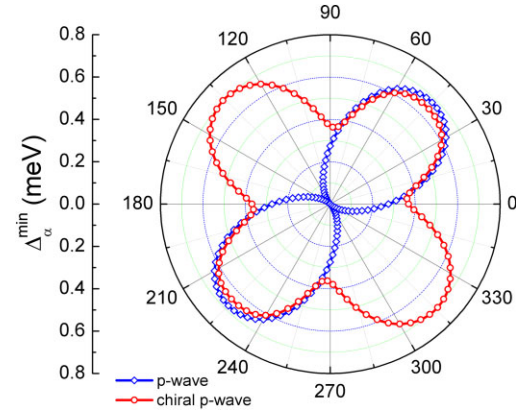

Figure 5 Chiral (open red circles) and non-chiral (open blue rhombuses) single-particle excitation energy gaps $\left[\Delta_\alpha^{min}(\theta)\right]$ at zero temperature as functions of the polar angle for the same superconductors as in Fig. 3.

explained by considering that $2\Delta_{nc}^2 > \Delta_c^2$ and for $\Delta_\alpha \ll |t|$ the minimum of $E_\alpha(k_x, k_y)$ occurs at the Fermi surface, $\varepsilon(\boldsymbol{k}) = \mu_\alpha$, which leads to $E_{nc}^2(k_F, k_F) - E_c^2(k_F, k_F) = 2(2\Delta_{nc}^2 - \Delta_c^2)\sin^2(k_F a) > 0$.

4 Conclusions In this work, we have studied within the BCS formalism both chiral and non-chiral p-wave superconducting states driven by an asymmetrical second-neighbor correlated hopping interaction due to a small orthorhombic distortion in the square lattice. Such asymmetry [$\delta_3 = (\Delta t_3^+ - \Delta t_3^-)/2$] breaks the degeneracy of p-wave superconducting states given by $+$ and $-$ in Eq. (12) for the chiral case, as well as in Eq. (13) for the non-chiral case. This leads to an energetic stabilization of one p-wave state for each case and then the physical properties of these lower energy states are comparatively investigated. The results

Figure 3 Chiral (open red circles) and non-chiral (open blue rhombuses) superconducting gaps (Δ_α) versus temperature (T) for the same systems of Fig. 2 with $n = 0.9$.

show that the chiral p-wave gap (Δ_c) is, in general, larger than the non-chiral one (Δ_{nc}). However, the electronic specific heat of the non-chiral superconducting state has a better agreement with the experimental data of Sr_2RuO_4.

In order to determine the symmetry of the ground superconducting state, we further calculated the Helmholtz free energy

$$F_\alpha = W_\alpha - TS_\alpha, \tag{19}$$

where

$$W_\alpha = \frac{1}{N_s} \sum_{\boldsymbol{k}} [\varepsilon(\boldsymbol{k}) - E_\alpha(\boldsymbol{k})] + \frac{1}{N_s} \sum_{\boldsymbol{k}} \frac{|\Delta_\alpha(\boldsymbol{k})|^2}{2E_\alpha(\boldsymbol{k})}$$
$$+ (n-1)\mu_\alpha - \frac{U}{4}n^2 \tag{20}$$

is the electronic energy per site and

$$S_\alpha = \frac{-2k_B}{N_s} \sum_{\boldsymbol{k}} \{[1 - f_\alpha(\boldsymbol{k})] \ln [1 - f_\alpha(\boldsymbol{k})]$$
$$+ f_\alpha(\boldsymbol{k}) \ln f_\alpha(\boldsymbol{k})\} \tag{21}$$

is the electronic entropy per site of the superconducting state. The numerical results show a difference between F_c and F_{nc} about 10^{-8} eV, which is of the same order of magnitude than the numerical error of our calculations. Hence, this free-energy analysis cannot distinguish if the p-wave super-conducting ground state is chiral or non-chiral. However, the specific heat analysis reveals only excitations from a non-chiral p-wave superconducting state, since the presence of line nodes leads to lower energy excitations from chiral and non-chiral almost degenerate ground states. In consequence, our results suggest that Sr_2RuO_4 has a non-chiral p-wave superconducting gap within the generalized Hubbard model.

References

[1] A. P. Mackenzie and Y. Maeno, Rev. Mod. Phys. **75**, 657 (2003).
[2] C. C. Tsuei and J. R. Kirtley, Rev. Mod. Phys. **72**, 969 (2000).
[3] K. D. Nelson, Z. Q. Mao, Y. Maeno, and Y. Liu, Science **306**, 1151 (2004).
[4] C. Kallin, Rep. Prog. Phys. **75**, 042501 (2012).
[5] T. Nomura and K. Yamada, J. Phys. Soc. Jpn. **71**, 1993 (2002).
[6] E. J. Rozbicki, J. F. Annett, J. Souquet, and A. P. Mackenzie, J. Phys.: Condens. Matter **23**, 094201 (2011).
[7] R. Matzdorf, Z. Fang, Ismail, J. Zhang, T. Kimura, Y. Tokura, K. Terakura, E. W. Plummer, Science **289**, 746 (2000).
[8] J. S. Millán, L. A. Pérez, and C. Wang, Phys. Lett. A **335**, 505 (2005).
[9] J. Hubbard, Proc. R. Soc. A **276**, 238 (1963).
[10] L. A. Pérez, J. S. Millán, and C. Wang, Int. J. Mod. Phys. B **24**, 5229 (2010).
[11] E. Dagotto, J. Riera, Y. C. Chen, A. Moreo, A. Nazarenko, F. Alcaraz, and F. Ortolani, Phys. Rev. B **49**, 3548 (1994).
[12] J. E. Hirsch and F. Marsiglio, Phys. Rev. B **39**, 11515 (1989).
[13] G. Rickayzen, Theory of Superconductivity (Wiley, New York, 1965), p. 146.
[14] V. P. Mineev and K. V. Samokhin, Introduction to Unconventional Superconductivity (Gordon and Breach, New York, 1999), p. 38.
[15] L. A. Pérez and C. Wang, Solid State Commun. **118**, 589 (2001).
[16] J. S. Millán, L. A. Pérez, and C. Wang, Physica C **408**, 259 (2004).
[17] P. Nozieres and S. Schmitt-Rink, J. Low Temp. Phys. **59**, 195 (1985).
[18] J. S. Millán, I. R. Ortiz, L. A. Pérez, and C. Wang, J. Phys.: Conf. Ser. **490**, 012221 (2014).
[19] J. E. Hirsch and F. Marsiglio, Phys. Rev. B **45**, 4807 (1992).
[20] M. Tinkham, Introduction to Superconductivity (McGraw-Hill, New York, 1996), p. 64.
[21] S. Nishizaki, Y. Maeno, and Z. Mao, J. Phys. Soc. Jpn. **69**, 572 (2000).